Assessing the Branching Architecture of Sparsely Branched Metallocene-Catalyzed Polyethylenes Using the Pompom Constitutive Model

Phillip J. Doerpinghaus and Donald G. Baird*

Department of Chemical Engineering, Virginia Polytechnic Institute and State University, Blacksburg, Virginia 24061-0211

Received August 15, 2002

ABSTRACT: The model parameters for the multimode differential pompom constitutive equation were determined for densely branched, sparsely branched, and linear polyethylene resins. The versatility and robustness of the pompom model is demonstrated through good rheological predictions in both shear and extensional deformations. The model parameters obtained for the sparsely branched materials indicate that the frequency of long-chain branching dominates the degree of strain hardening observed in uniaxial extension. This finding agrees well with the proposed mechanism of long-chain branching using constrained-geometry metallocene catalysts. The model parameters agree qualitatively with the long-chain branch content determined from dilute solution measurements. Furthermore, the values of the number of pompom arms (i.e., the priority) were found to be quite high even for the sparsely branched materials but were only associated with the longest relaxation times. This suggests that branching for the metallocene systems may be highly concentrated on the longest chains rather than randomly distributed on all of the chains.

Introduction

The recent development of the "pompom" constitutive model of McLeish and Larson[1] has provided new insight into the subtle effects of long-chain branching on the rheological properties of branched polyethylenes. McLeish and Larson demonstrate that the constitutive model predictions under shear and extensional deformations resemble the observed rheological response of densely branched polyethylene resins. Most notably, the model correctly predicts strain hardening in both uniaxial and planar extensional flows. Furthermore, the model parameters used to fit available rheological data can be used to construe some idea of the molecular structure as well as the extent of branching. In the case of the densely branched, low-density polyethylene (LDPE), the pompom model seems well suited. However, its application to sparsely branched commercial systems has gone untested. The development of sparsely branched metallocene-catalyzed polyethylene resins using constrained geometry catalysts (CGC) represents a new benchmark with which to test the versatility of the pompom model while assessing the architecture of these systems.

The application of the pompom model to densely branched materials such as commercial low-density polyethylene (LDPE) was recently undertaken by Inkson et al.[2] Using a series of well-characterized LDPE resins, the authors were able to fit shear and extensional data with considerable accuracy using a multimode formulation of the pompom differential model. Surprisingly, transient shear viscosity predictions agreed well with experimental measurements using material parameters determined solely from shear dynamic oscillatory and transient extensional data. Subsequent model modifications by Blackwell et al.[3] provided smoother, more accurate predictions to transient and steady extensional viscosity predictions of the same LDPE resins.

The success of the model in predicting the rheological response of LDPE relies upon the idea that segmental tension can be traced from the free ends at the surface of the macromolecule inward toward the core.[4] The maximum accumulated segmental tension is determined by its *priority*,[5] and the rate of relaxation of that stress is determined by its *seniority*.[6] In effect, this concept associates the fastest relaxing constitutive modes to the free arms and the slowest relaxing modes to the core segments. This approach is tantamount to deconstructing, or decoupling, the macromolecular superstructure into an ensemble of pompom molecules. The results of this treatment provide accurate results for densely branched low-density polyethylene.[2,3,36]

The extension of the pompom model to sparsely branched systems presents a different challenge. The degree of branching found in sparsely branched metallocene polyethylene is considerably less than that formed from free radical polymerization. The proposed mechanism for branching in metallocene polyethylenes occurs by temperature-activated, β-hydride elimination reactions that give rise to vinyl-terminated polymer chains.[7] These *macromonomers* can then be re-incorporated into growing chains, thereby generating long chain branches. It is believed that sparsely branched metallocene polyethylene resins consist of a mixture of linear, star, and higher branched species.[8,9] The results of modeling the coordination polymerization of ethylene using CGC catalysts like those developed by the Dow Chemical Co.[10] suggest that the weight fraction of macromolecules having two or more branch points accounts for a relatively small mass of the whole polymer. As a result, one would expect very few molecular segments capable of being described by a branched pompom molecule. This contrasts greatly with the situation observed for highly branched LDPE discussed above.

* To whom all correspondence should be addressed. Phone: (540) 231-5998. Fax: (540) 231-5022.

10.1021/ma021332m CCC: $22.00
Published on Web 12/07/2002

The accuracy of the pompom model predictions and the precision of the model parameters are dependent upon the quality and breadth of the fitted rheological data. This is certainly true when differentiating varying degrees of long-chain branching in LDPE or mPE resins. Prior studies of commercial and model polymer systems have shown that rheological characterization is a sensitive indicator of molecular structure.[11−14] More specifically, studies using model polymer systems have shown that the degree, length, and structure (i.e., star, comb, random, etc.) of branching have considerable effect on the zero-shear viscosity and the onset of shear-thinning behavior.[15−17] However, various combinations of molecular weight and long-chain branching can lead to similar shear rheological behavior.[18] This complication is often observed in commercial materials and requires alternate rheological measurements to differentiate the effects of branching.[19,20]

In addition to shear deformations, extensional deformations can be used to assess the effects of molecular structure on rheology. In fact, extensional rheological characterization has also been found to be sensitive to long-chain branching.[21] Unlike linear polymers, which exhibit shear and extensional-thinning behavior, long-chain branched polymers often show extensional viscosity growth above the linear viscoelastic (LVE) limit of $3\eta^+(t)$. This rise above the LVE envelope is generally referred to as *strain hardening*. Previous studies on linear and branched polyethylenes have shown that the presence and magnitude of strain-hardening behavior are dependent upon the degree and topology of long-chain branching present.[22−25] More recently, Bin Wadud and Baird[20] have shown that this is also qualitatively true for sparsely branched metallocene polyethylene resins. In contrast, Kasehagen and Macosko[26] have argued that extensional strain hardening is simply a result of extremely long relaxation times not readily observed in shearing flows and that the observed rheological response may or may not be attributed to the presence of long-chain branching in randomly branched polybutadienes.

Although extensional measurements of model systems are often difficult to obtain, the results indicate the importance of branch structure over the degree of branching. The extensional measurements of polymer melts are notoriously difficult to obtain.[27] The presence of a free surface often leads to nonhomogeneous flow and the need for numerous measurements at each extension rate. In the case of model systems, this often prohibits extensional characterization because of the small quantity of material available. However, research suggests that more than one branch point per chain is required for extensional strain hardening.[28−30,37] Ye and Sridhar[28] measured the extensional viscosity of three-arm polystyrene solutions and found that extensional thinning was observed over a very wide range of extension rates. These observations were found to be qualitatively similar to those of the linear polymer solutions. On the other hand, McLeish et al.[29] and Lohse et al.[30] found that only molecules having multiple branch points exhibit extensional strain hardening behavior. McLeish et al.[29] observed extensional strain hardening in a model, H-shaped polyisoprene (PI), while Lohse et al.[30] observed it for comb-branched hydrogenated polybutadienes (HPB). Furthermore, Lohse et al. determined that a very small amount, as little as 5%, of the comb-branched HPB blended with linear polyethylene was required to affect the extensional viscosity. These rather few observations clearly imply that extensional viscosity measurements can be used to assess the degree and possibly the type of long-chain branching that exists in sparsely branched metallocene polyethylenes.

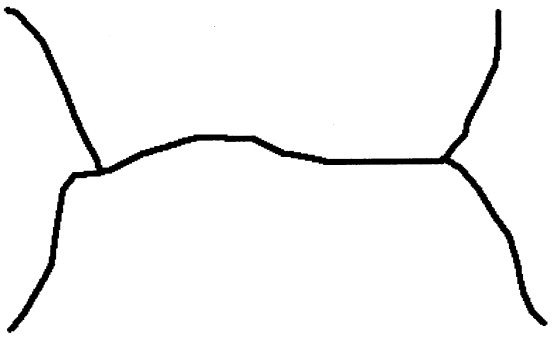

Figure 1. Schematic representation of the simplest pompom molecule, the H-polymer ($q = 2$).

In the present study, a series of five commercially available polyethylene resins is investigated. Three of the five resins are narrow molecular weight distribution, sparsely branched metallocene polyethylenes (mPE) that are the focus of this study. Each of these mPE resins contains a different degree of long-chain branching as determined from dilute solution analysis. In addition to the sparsely branched mPE resins, a linear low-density polyethylene (LLDPE) resin and a densely branched LDPE is also used. These conventional resins are used to test the versatility of the pompom model in the cases of considerable long-chain branching and no long-chain branching. The goal of this study is to determine whether the structure of sparsely branched metallocene polyethylene predicted using the pompom molecular constitutive equation is consistent with the proposed mechanism for long-chain branching during polymerization and the level of branching obtained from dilute solution measurements. Using available shear and extensional rheological data, a set of model parameters are fitted for each of the polyethylene resins investigated. From these model parameters, characteristic pompom structures are deduced.

The Pompom Constitutive Model

In this section, a brief review of the constitutive model and the basic set of equations used to predict the shear and extensional rheological responses are presented. Although a rigorous derivation of the original model is quite insightful, these details can be found elsewhere.[1] The pompom molecule is a relatively simple structure consisting of two q-armed stars connected by a single backbone section known as the crossbar (Figure 1). Using a generalization of the Doi−Edwards tube model,[31] the configuration of these pompom molecules can be described by two dynamic variables $\mathbf{S}$ and λ. The tensor $\mathbf{S}$ describes the average backbone tube orientation and the scalar λ describes the average backbone stretch. Furthermore, the time scales for backbone orientation and stretch are determined by two separate relaxation times, τ_b and τ_s, respectively. The maximum backbone stretch, and thus the maximum accumulated stress, is determined by the number of pompom arms, q. For this particular treatment, the effects of arm withdrawal in the original formulation have been neglected.[1]

The evolution of the dynamic variables $\mathbf{S}$ and λ are governed by the differential equations appearing in

Table 1. Differential Pompom Constitutive Model Equation Set

stress	$\sigma = \sum_i \sigma_i = 3\sum_i g_i \lambda_i^2 \boldsymbol{S}_i$	(1)
orientation	$\boldsymbol{S}_i = \boldsymbol{A}_i / \mathrm{tr}\boldsymbol{A}_i$	(2a)
	$(D/Dt)\boldsymbol{A}_i = \boldsymbol{K}\cdot\boldsymbol{A}_i + \boldsymbol{A}_i\cdot\boldsymbol{K}^T - (1/\tau_{bi})(\boldsymbol{A}_i - \boldsymbol{I})$	(2b)
stretch	$(D/Dt)\lambda_i = \lambda_i(\boldsymbol{K}:\boldsymbol{S}_i) - (1/\tau_{si})(\lambda_i - 1)e^{\nu_i^*(\lambda_i - 1)}$	(3)

Table 2. Molecular Weight, MFI, and LCB Content of the Materials Studied

resin	MFI, dg/min	M_w	M_w/M_n	M_z	LCB, 10^4 C
Exact 0201	1.1	88 700	2.14	158 900	0.79
Exact 3132	1.2	111 000	2.04	180 400	
Affinity PL1840	1.0	87 400	2.43	160 200	0.57
Affinity PL1880	1.0	115 800	2.12	183 700	0.18
NA952	2.0	235 500	17.1	2 619 300	39[a]
NTX101	0.9	122 700	3.44	319 700	

[a] C^{13} NMR measurement.

Table 1 and the resulting extra stress tensor $\boldsymbol{\sigma}$ is calculated from these variables. The differential approximation for **S** has been chosen for this study because it not only provides a similar asymptotic behavior to the full integral form[1] but also provides analytical solutions for the orientation tensor components under homogeneous flow conditions. The backbone stretch evolution equation incorporates the concept of drag−strain coupling of the branch point as proposed by Blackwell and co-workers.[3] In this case, the parameter ν^* has been approximated by the suggested value of $2q^{-1}$. A multimode formulation has been implemented for this study, and thus each mode will have four unknown parameters: the backbone orientation time τ_{bi}, the individual contribution to the plateau modulus g_i, the number of pompom arms q_i, and the backbone stretch orientation time τ_{si}. These unknown parameters are determined from fitting available shear and extensional rheological data.

The recommended procedure by Inkson et al.[2] has been used to determine the model parameters in this study. First, the backbone orientation times (τ_{bi}) and individual plateau moduli (g_i) are determined from linear viscoelastic measurements. This is accomplished using a least-squares fit to available data. In this case, the choice of τ_{bi} is arbitrary and one constitutive mode per decade of shear rate was used. Second, the number of pompom arms and the stretch orientation time are determined from transient tensile growth measurements. This particular fitting process usually requires a trial-and-error approach. Fortunately, only those modes active at a given extension rate ($\tau_{si}\mathbf{f} \sim 1$) are affected. Fitting the slowest extension rate first and proceeding to higher rates generally provides the best results.

Experimental Section

Materials. The five polyethylene resins employed for this study are commercially available materials. Table 2 lists each of the resins considered along with their molecular characteristics as determined by dilute solution measurements. The two Dow Affinity resins are ethylene-octene copolymers produced using the INSITE catalyst technology. These particular metallocene resins have been investigated in a previous study.[20] The ExxonMobil Exact 0201 resin is an ethylene-octene copolymer produced using the EXXPOL catalyst technology. The conventional LLDPE (NTX101) is an ethylene−hexene copolymer also manufactured by ExxonMobil using conventional Ziegler−Natta catalysts. The conventional LDPE (NA952) is manufactured by Equistar and is produced using a tubular free-radical polymerization process. None of the resins listed contain any additional additives other than the standard antioxidant packages.

The degree of long-chain branching determined from dilute solution measurements, using a combination of GPC, light scattering, and intrinsic viscosity measurements as discussed in ref 13, are reported in Table 2. The sparsely branched mPE resins vary in content from 0.18 to 0.79 LCB/10^4 carbons. This is well over an order of magnitude less than the branching content reported for the conventional LDPE resin (NA952) using C^{13} NMR measurements. Although C^{13} NMR measurements may include some short-chain branches,[32] the breadth of distribution exhibited by NA952 is indicative of a high degree of long-chain branching.[33] The NTX101 resin is a linear polyethylene copolymer and was not analyzed for branch content.

Shear Rheological Measurements. The shear rheological measurements for each resin were determined using a Rheometrics Mechanical spectrometer model 800 (RMS-800). The dynamic oscillatory data were collected over the range of 0.1−100 rad s^{-1} using 25 mm parallel plate fixtures. The steady shear rheological measurements were collected over a range of 0.001−1.00 s^{-1} using a 25 mm cone and plate fixture. Stress growth measurements were carried out at shear rates varying from 0.001 to 1.0 s^{-1}. For shear rates greater than 0.3 s^{-1} edge fracture was observed for strains greater than 100 and measurements were stopped. The cone angle used for all steady shear measurements was 0.1 rad. All testing was performed within an inert nitrogen atmosphere to prevent thermooxidative degradation. In most cases, the test samples were prepared by compression molding preforms at 170 °C under nominal pressure and allowing them to cool slowly. All steady shear measurements were carried out at a test temperature of 150 °C. The dynamic oscillatory shear moduli data were collected over a range of temperatures and shifted to a reference temperature of 150 °C.

The results presented represent an average of at least three runs using different samples each time. The calculated error for the dynamic oscillatory and steady shear measurements was found to be no greater than ±5 and ±10%, respectively.

Extensional Rheological Measurements. Transient uniaxial extensional measurements were obtained using a Rheometrics extensional rheometer, model 9000 (RER-9000). This particular extensional rheometer is based upon the rod-pulling design suggested by Münstedt.[34] The transient extensional data were collected over the extension rate range 0.01−1.00 s^{-1}. The maximum Hencky (true) strain achievable with this device is approximately 3.0 using test specimens with initial nominal lengths of 22 mm. The cylindrical test specimens were compression molded from polymer pellets at 170 °C under nominal pressure and allowed to cool slowly. They were then bonded to test clips using high-temperature UHU epoxy, mounted to the rheometer, and immersed in a neutraly buoyant silicone oil bath at 150 °C. Once thermal equilibrium was achieved, an applied extension rate deformed the sample and the resulting force was monitored using a leaf spring−LVDT assembly. When nonuniform deformation was visually observed, the acquired sample was discarded and an additional test was performed on a separate specimen.

The results presented for each extension rate represent an average of at least three runs using different samples each time. The calculated error for the extensional viscosity data varies between materials and depends on the achieved strain. The branched polyethylene resins showed the greatest degree of reproducibility with no more than 10% deviation up to the maximum Hencky strain achievable. The linear resin was much more problematic. The calculated error from $\epsilon_H = 0$ to 2.0 was found to be less than 10%, but above 2.0 strain units, homogeneous deformation was difficult to achieve at higher extension rates. In most cases, the extensional rheological data for the NTX101 resin was simply truncated above $\epsilon_H = 2.0$.

Results and Discussion

Linear Viscoelastic Data. The linear viscoelastic data are presented in Figures 2−4. Figure 2 illustrates

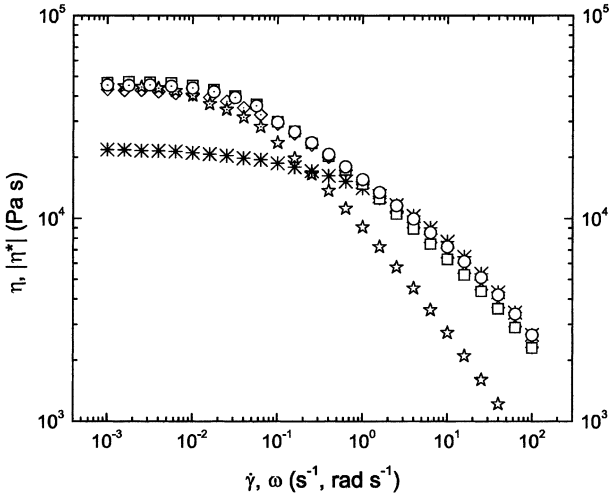

Figure 2. Steady shear and complex viscosities at 150 °C: (◇) Exact 0201, (☆) NA952, (∗) NTX101, (□) Affinity PL1840, and (○) Affinity PL1880. Symbols with a dot in the middle represent steady shear measurements; open symbols represent dynamic oscillatory measurements.

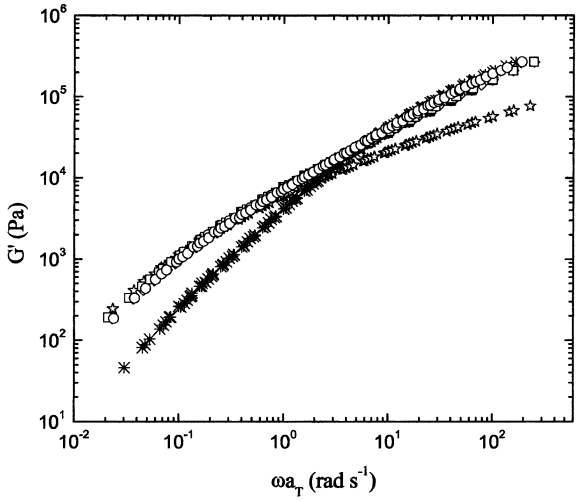

Figure 3. Storage moduli at T_{ref} = 150 °C: (◇) Exact 0201, (☆) NA952, (∗) NTX101, (□) Affinity PL1840, and (○) Affinity PL1880.

the observed shear viscosity flow curves for each of the resins over five decades in shear rate. Steady shear measurements were found to overlap well with dynamic oscillatory data in the range of rates investigated here. Figures 3 and 4 summarize the shear loss and storage moduli obtained for each resin at the shifted reference temperature of 150 °C. Together, these data were then used to determine the linear viscoelastic relaxation spectra as described previously. The arbitrarily chosen values for τ_{bi}, and the fitted values of g_i obtained from a numerical error-minimizing routine, can be found in Tables 3−7.

One of the greatest limitations observed during parameter fitting of τ_{bi} and g_i parameters was the lack of adequate low frequency data. This was certainly true for the branched materials that exhibited shear-thinning behavior at rates less than 0.01 s^{-1}. As a result, steady shear data were often used in combination with the dynamic data to fit the model parameters over the five decades of deformation rates. Despite this approach, it was later determined that an additional mode corresponding to $\tau_{bi} = 10^3$ s was required to accurately fit

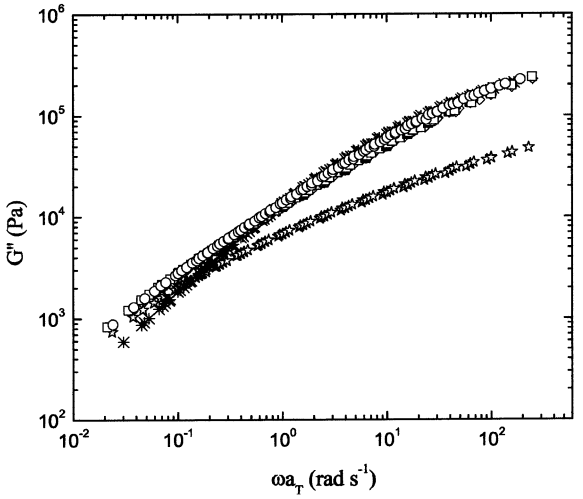

Figure 4. Loss moduli at T_{ref} = 150 °C: (◇) Exact 0201, (☆) NA952, (∗) NTX101, (□) Affinity PL1840, and (○) Affinity PL1880.

Table 3. Pompom Model Parameters for NA952

τ_{bi}	g_i	q_i	τ_{bi}/τ_{si}
10^{-2}	6.07×10^4	1	3.0
10^{-1}	2.28×10^4	1	3.0
10^{0}	7.90×10^3	1	3.0
10^{1}	1.88×10^3	7	2.5
10^{2}	1.10×10^2	12	1.3
10^{3}	5.20×10^0	20	1.0

Table 4. Pompom Model Parameters for Exact 0201

τ_{bi}	g_i	q_i	τ_{bi}/τ_{si}
10^{-2}	2.56×10^5	1	10
10^{-1}	4.55×10^4	1	10
10^{0}	1.21×10^4	1	10
10^{1}	1.82×10^3	1	10
10^{2}	7.23×10^1	11	3.5

Table 5. Pompom Model Parameters for Affinity PL1840

τ_{bi}	g_i	q_i	τ_{bi}/τ_{si}
10^{-2}	2.46×10^5	1	10
10^{-1}	4.90×10^4	1	10
10^{0}	1.06×10^4	1	10
10^{1}	2.02×10^3	1	10
10^{2}	7.61×10^1	10	4.0

Table 6. Pompom Model Parameters for Affinity PL1880

τ_{bi}	g_i	q_i	τ_{bi}/τ_{si}
10^{-2}	2.08×10^5	1	10
10^{-1}	5.50×10^4	1	10
10^{0}	9.88×10^3	1	10
10^{1}	2.01×10^3	1	10
10^{2}	6.35×10^1	7	8.0

Table 7. Pompom Model Parameters for NTX101

τ_{bi}	g_i	q_i	τ_{bi}/τ_{si}
10^{-2}	1.49×10^5	1	10
10^{-1}	9.05×10^4	1	10
10^{0}	6.43×10^3	1	10
10^{1}	3.53×10^2	1	10
10^{2}	2.25×10^1	1	10

the lowest extension rate data for the densely branched NA952 resin. This extremely long relaxation mode is not readily measured in shearing flows (because long times are required to obtain these data leading to degradation of the polymer), and its observation in extensional flow is in partial agreement with the findings of Kasehagen and Macosko.[26]

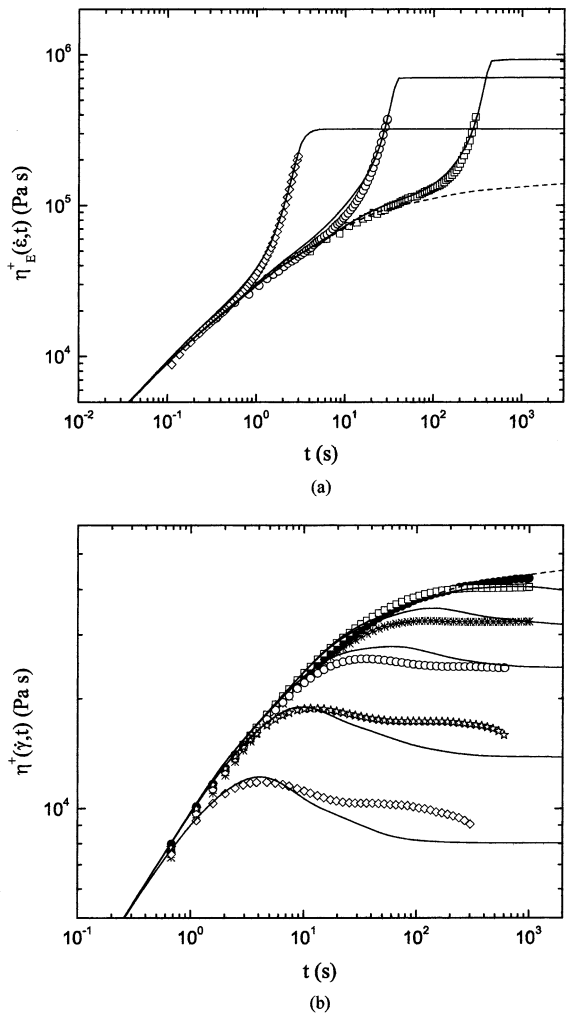

Figure 5. Transient (a) extensional and (b) shear viscosity growth curves for NA952: (●) $\dot{\epsilon},\dot{\gamma} = 0.001$ s^{-1}, (□) $\dot{\epsilon},\dot{\gamma} = 0.01$ s^{-1}, (∗) $\dot{\epsilon},\dot{\gamma} = 0.0316$ s^{-1}, (○) $\dot{\epsilon},\dot{\gamma} = 0.1$ s^{-1}, (☆) $\dot{\epsilon},\dot{\gamma} = 0.316$ s^{-1}, and (◇) $\dot{\epsilon},\dot{\gamma} = 1.0$ s^{-1}. Solid lines represent model predictions. Dashed lines are LVE growth curves.

Densely Branched Structures. To establish the consistency of the technique used in this study with those used in prior studies by Inkson et al.[2] and Blackwell et al.,[3] a densely branched LDPE resin is examined first. The experimental and predicted transient extensional and shear growth curves for NA952 are featured in Figure 5. The corresponding values of the q_i and τ_{bi}/τ_{si} obtained from fitting the extensional curves at extensional rates of 0.01, 0.1, and 1.0 s^{-1} are shown in Table 3. The predicted transient extensional viscosities found in Figure 5a agree quite well with measured values. The onset and degree of strain hardening are captured quite well for all three of the rates presented. The only uncertainties from this treatment are the values of q_i. Because steady-state extensional viscosities were not obtained up to the maximum Hencky strain of 3.0, the actual value of q_i for each mode could not be established. Therefore, the minimum values of q_i that provide acceptable fits to the rheological data have been reported here. The true values of q_i may in fact be higher.

The predicted transient shear viscosities are found in Figure 5b. The level of agreement is quite good considering the model parameters have been optimized for uniaxial extensional data. The predicted steady-state viscosities agree well with experimental data in the low shear rate range from 0.001 to 0.1 s^{-1}and begin to deviate by as much as 20% at the higher rates. On the other hand, the departure from the LVE limiting curve and the observed magnitude of the stress overshoot appear to be more accurate at higher rates.

The results obtained for the densely branched polyethylene used in this study are consistent with the trends observed by Inkson et al.[2] and Blackwell et al.[3] in similar LDPE resins. The model parameters determined from extension are descriptive of a highly branched low density-polyethylene resins. Surprisingly, the overall fits for transient extensional and shear rheological data are quite good despite the use of fewer pompom modes than either Inkson et al. or Blackwell et al. used in their studies. The maximum number of modes used in this study was six modes for the LDPE with the remaining four resins being modeled by only five modes. Although this may lead to a greater degree of response averaging across the modes, this treatment best reflects the amount of rheological data available for these systems.

Sparsely Branched Structures. Having analyzed a densely long-chain branched system, it now seems logical to turn our attention to sparsely branched resins. As stated before, the sparsely branched resins are believed to represent a collection of discrete linear, star, and pompom shaped molecules. As such, the degree of strain hardening is expected to be less and the number of branched pompom modes is expected to be few. In this subsection, the pompom model predictions for the three sparsely branched metallocene resins listed in Table 2 will be presented.

On the basis of dilute solution measurements, the Exact 0201 material features the greatest degree of branching of the metallocene resins at 0.79 LCB/10^4 carbons. As noted earlier, this is more than an order of magnitude less that the branching content observed in the densely branched LDPE system. The experimental and predicted transient extensional and shear viscosity growth curves are presented in Figure 6. The corresponding values of the q_i and τ_{bi}/τ_{si} are tabulated in Table 4. The transient extensional viscosity predictions agree quite well with the experimental data. The constitutive model accurately captures the onset and magnitude of strain-hardening behavior. Furthermore, the transient shear predictions are surprisingly accurate. Once again, the model parameters have been optimized for the extensional measurements. The fitted parameters clearly indicate that only one branched pompom mode is present and that its effects are evident at $\dot{\epsilon} = 1.0$ s^{-1}. In fact, the magnitude of q_i for the longest relaxing mode was accurately determined from the maximum in the extensional viscosity data at $\dot{\epsilon} = 1.0$ s^{-1}. On the other hand, the relaxation time ratio τ_{bi}/τ_{si} was determined from the transient extensional viscosity data at $\dot{\epsilon} = 0.1$ s^{-1}. Both of these led to excellent predictions at the smallest extension rate of $\dot{\epsilon} = 0.01$ s^{-1}.

The predicted transient growth curves for Affinity PL1840 are illustrated in Figure 7. The transient extensional predictions are not as accurate at low extension rates, predicting more strain hardening than observed experimentally. Furthermore, at the highest extension rate, the observed onset of strain hardening occurs sooner than predicted. This, of course, may be a consequence of having a single branched pompom mode active over two decades in extension rate. The model

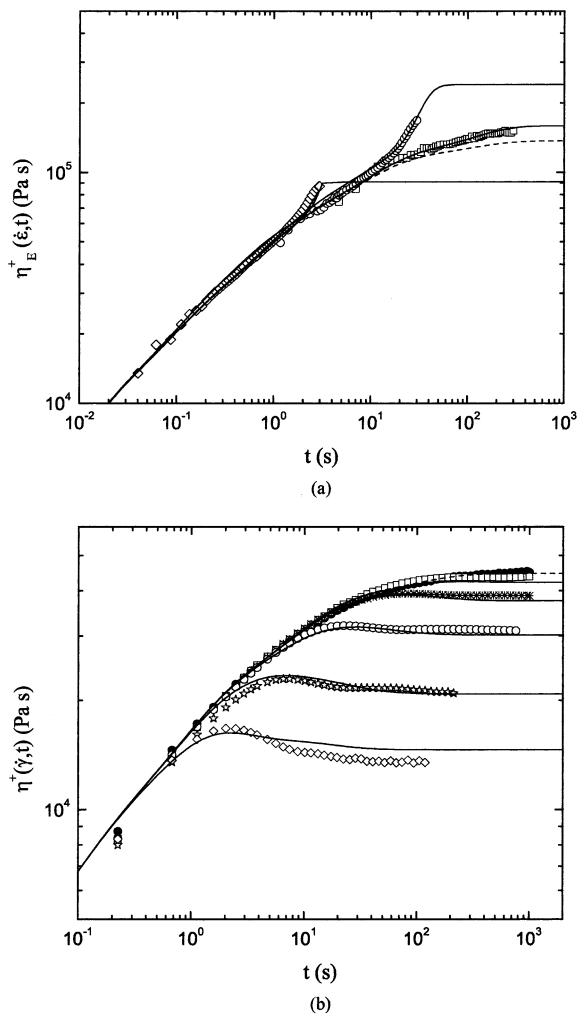

Figure 6. Transient (a) extensional and (b) shear viscosity growth curves for Exact 0201: (●) $\dot{\epsilon},\dot{\gamma} = 0.001$ s^{-1}, (□) $\dot{\epsilon},\dot{\gamma} = 0.01$ s^{-1}, (∗) $\dot{\epsilon},\dot{\gamma} = 0.0316$ s^{-1}, (○) $\dot{\epsilon},\dot{\gamma} = 0.1$ s^{-1}, (☆) $\dot{\epsilon},\dot{\gamma} = 0.316$ s^{-1}, and (◇) $\dot{\epsilon},\dot{\gamma} = 1.0$ s^{-1}. Solid lines represent model predictions. Dashed lines are LVE growth curves.

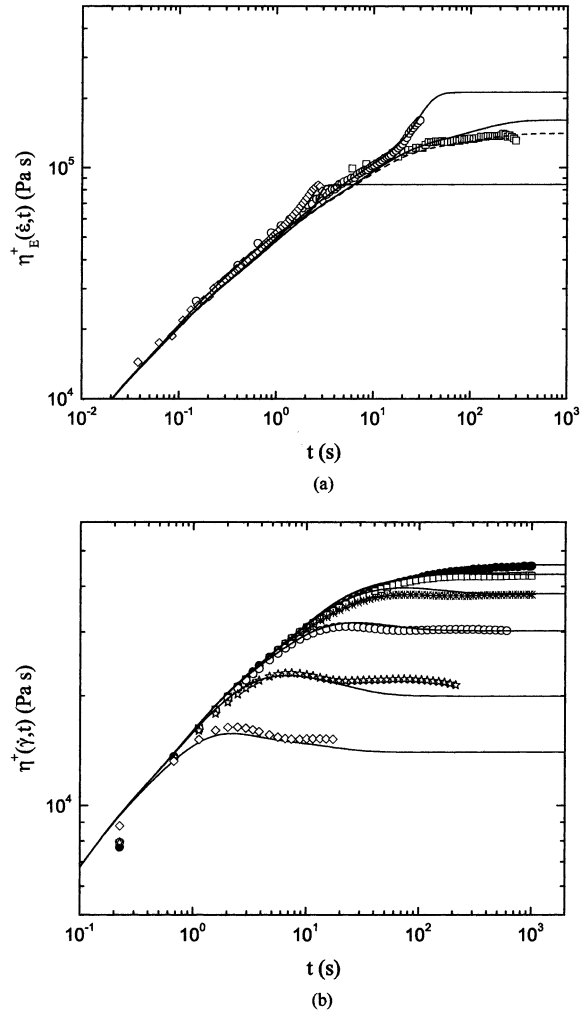

Figure 7. Transient (a) extensional and (b) shear viscosity growth curves for Affinity PL1840: (●) $\dot{\epsilon},\dot{\gamma} = 0.001$ s^{-1}, (□) $\dot{\epsilon},\dot{\gamma} = 0.01$ s^{-1}, (∗) $\dot{\epsilon},\dot{\gamma} = 0.0316$ s^{-1}, (○) $\dot{\epsilon},\dot{\gamma} = 0.1$ s^{-1}, (☆) $\dot{\epsilon},\dot{\gamma} = 0.316$ s^{-1}, and (◇) $\dot{\epsilon},\dot{\gamma} = 1.0$ s^{-1}. Solid lines represent model predictions. Dashed lines are LVE growth curves.

parameters appearing in Table 5 were again determined from the maximum viscosity observed at $\dot{\epsilon} = 1.0$ s^{-1} and the transient growth form at $\dot{\epsilon} = 0.1$ s^{-1}. Surprisingly, the number of pompom arms determined for the slowest relaxing mode is essentially the same as that for the Exact 0201 resin. This occurs despite differences in the dilute solution measurements of long-chain branching content and the noticeably reduced degree of strain-hardening behavior at an extension rate of 0.01 s^{-1}. Regardless, the transient shear viscosity curves are reasonably accurate over the range covered.

The Affinity PL1880 resin contains the least amount of long-chain branching according to dilute solution measurements and consequently does not exhibit a substantial degree of strain-hardening behavior. This reduced response makes it difficult to accurately gage the effectiveness of the pompom model's fitting ability to the data presented in Figure 8. In fact, the material response at $\dot{\epsilon} = 0.01$ s^{-1} appears to be strain softening with respect to $3\eta^+(t)$. Despite concern regarding the sensitivity of the pompom model to fit the response exhibited by the Affinity PL1880, the same method employed for the previous two materials was used. The model parameters obtained from fitting the four linear and one branched pompom modes are summarized in Table 6. Again one observes that the number of pompom arms is still relatively large at a value of seven, but the relaxation time ratio has increased to a value of 8. This is at least a factor of 2 greater than those reported for either Exact 0201 or PL1840. Clearly, the separation in time scales appears to be the dominating factor for predicting strain-hardening behavior in sparsely branched mPE resins.

The model predictions obtained for sparsely branched metallocene resins agree qualitatively well with both transient extensional and shear viscosity measurements. The observed strain-hardening behavior that arises from as few as 0.18 LCB/10^4 carbons is modeled well using a set of linear and branched pompom structures. The fitted model parameters appearing in Tables 4−6 show that only one branched pompom mode exists in each of the parameter sets and that this mode is represented by the longest relaxation time. It is recognized that if more relaxation times were used other long relaxation times could also have some branched modes associated with them. Furthermore, the fitted parameters imply that the separation in orientation and stretch time scales is equally, if not more, important in describing the observed extensional strain-hardening behavior as is the number of pompom arms, q_i. The implications arising from these model parameters are discussed in a later section.

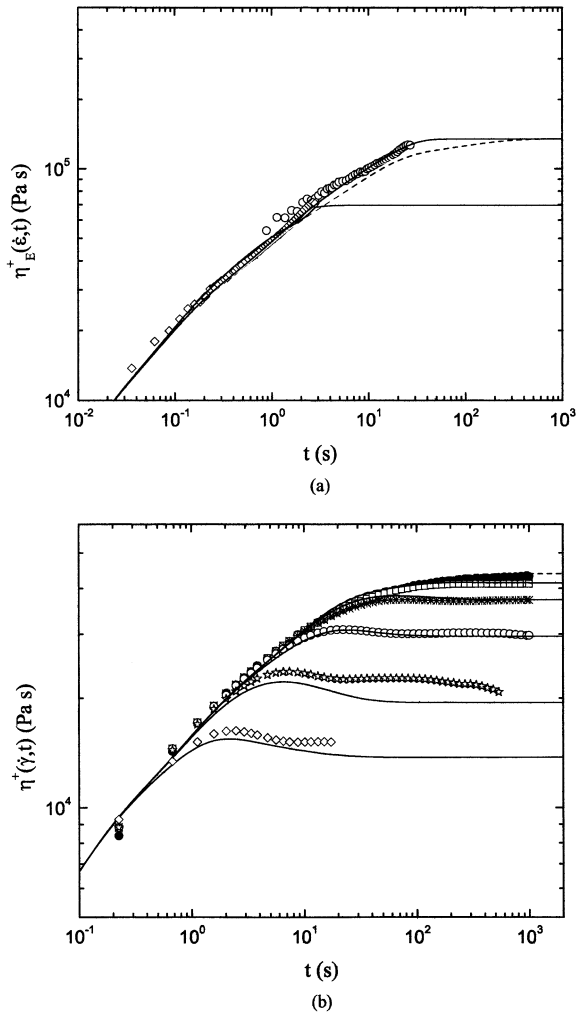

Figure 8. Transient (a) extensional and (b) shear viscosity growth curves for Affinity PL1880. (●) $\dot{\epsilon},\dot{\gamma} = 0.001$ s^{-1}, (□) $\dot{\epsilon},\dot{\gamma} = 0.01$ s^{-1}, (XXXXX) $\dot{\epsilon},\dot{\gamma} = 0.0316$ s^{-1}, (○) $\dot{\epsilon},\dot{\gamma} = 0.1$ s^{-1}, (☆) $\dot{\epsilon},\dot{\gamma} = 0.316$ s^{-1}, (◇) $\dot{\epsilon},\dot{\gamma} = 1.0$ s^{-1}. Solid lines represent model predictions. Dashed lines are LVE growth curves.

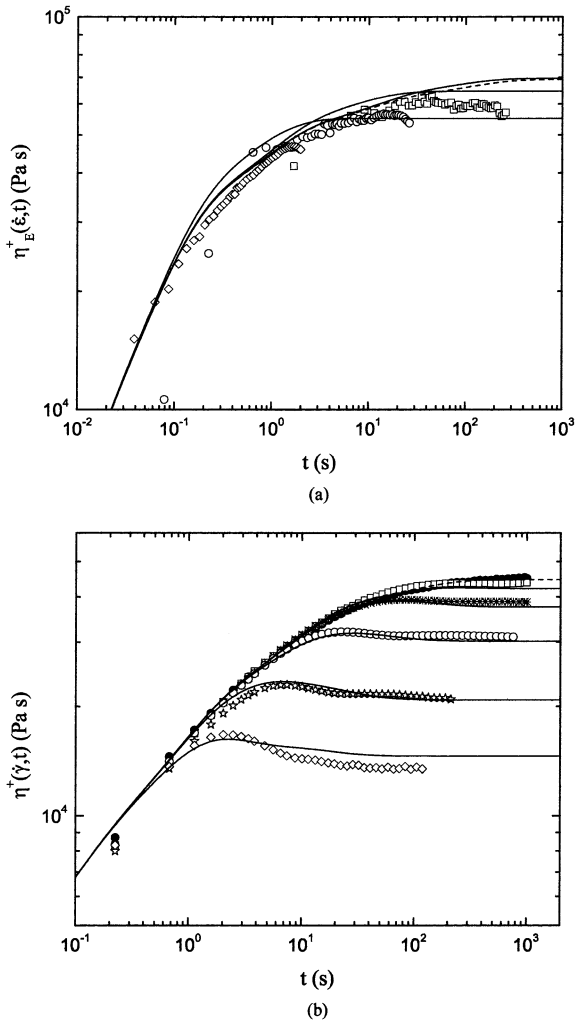

Figure 9. Transient (a) extensional and (b) shear viscosity growth curves for NTX101: (●) $\dot{\epsilon},\dot{\gamma} = 0.001$ s^{-1}, (□) $\dot{\epsilon},\dot{\gamma} = 0.01$ s^{-1}, (∗) $\dot{\epsilon},\dot{\gamma} = 0.0316$ s^{-1}, (○) $\dot{\epsilon},\dot{\gamma} = 0.1$ s^{-1}, (☆) $\dot{\epsilon},\dot{\gamma} = 0.316$ s^{-1}, and (◇) $\dot{\epsilon},\dot{\gamma} = 1.0$ s^{-1}. Solid lines represent model predictions. Dashed lines are LVE growth curves.

Linear Structures. Although the pompom constitutive model has been specifically designed to address the rheological effects of long-chain branching, the linear case may be equally important. This can of course be accomplished by setting the number of pompom arms equal to one. However, in the light of the results obtained from the sparsely branched systems, one could also increase the separation in orientation and stretch time scales to an infinite extent thereby decreasing or negating the predicted degree of extensional strain hardening. Therefore, one would assume that accurate modeling of linear materials is important as the degree of long-chain branching becomes very small.

To test the versatility of the pompom model, a conventional linear low-density has been considered. The molecular characteristics of the linear NTX101 resin can be found in Table 2. The rheological data and corresponding pompom model predictions can be found in Figure 9. Knowing that this Ziegler−Natta polymerized resin has no long-chain branches, the choice of nonlinear parameters becomes trivial. The value of q_i is set to one for all modes and the relaxation time scale ratios become inconsequential (or approach infinity). Beginning with the transient shear predications in Figure 9b, the predicted results are quantitatively good. The onset of thinning behavior, magnitude of the viscosity overshoot, and steady-state viscosity are well predicted. On the other hand, the extensional viscosity prediction exhibits some anomalous behavior. Clearly, the experimental data plotted in Figure 9a grow with $3\eta^+(t)$ and deviate negatively at some critical value of the applied Hencky strain. The predictions, on the other hand, clearly indicate an initial degree of strain hardening before reaching steady state. This numerical artifact has been attributed to the approximating form of the differential pompom constitutive model.[35] The full integral form of the pompom model does not suffer from this anomaly.

The pompom predictions for linear polyethylene melts are very accurate in shear flows. This is not surprising because of the greater dependence upon chain orientation rather than stretch. As a result, the transient shear and extensional characteristics can be determined solely from linear viscoelastic data. Unfortunately, the differential form of the pompom model gives rise to physically unrealistic predictions in extensional deformations. This artifact will have very little effect on the predictions of highly branched systems, but may become important when dealing with predominantly linear systems or systems in which the branched species do not contribute to strain hardening behavior (i.e., star-branched polymers).

Interpretation of Suggested Pompom Structures. The model parameters obtained for the sparsely branched metallocene polyethylenes suggest that the observed degree of extensional strain hardening is more sensitive to the separation in orientation and stretch time scales as evidenced by τ_{bi}/τ_{si} than the number of pompom arms, q_i. A decrease in the reported long-chain branch content from 0.79 to 0.18 LCB/10^4 carbons for Exact 0201 and Affinity PL1880 results in a 36% decrease in q_i and a 128% increase in τ_{bi}/τ_{si}. This observation indicates that the molecular dependence of τ_{bi}/τ_{si} is the dominating factor for assessing an average branched structure.

According to the original derivations by McLeish and Larson,[1] the relaxation time scale ratio is directly proportional to the product of the normalized crossbar molecular weight and the fraction of the total molecular weight contained within the crossbar

$$\frac{\tau_{bi}}{\tau_{si}} \propto s_b \phi_b \tag{1}$$

Thus, an increase in the effective distance between branch points will increase the time scale separation. This premise appears to be consistent with the long-chain branching mechanism described earlier. That is, the frequency of β-hydride elimination reactions during polymerization will determine the frequency of, or molecular weight between, long-chain branches. Therefore, the greater the number of branch points for a given molecular weight, the lower the molecular weight between branch points and the smaller the relaxation time scale ratio. This trend agrees qualitatively with the dilute solution measurements of the degree of branching obtained for the metallocene polyethylenes.

One interesting result taken from the same model parameters was the large value of q_i determined for the longest relaxing mode. The observed magnitudes of q_5 ranged from 11 for the Exact 0201 resin to 7 for the Affinity PL1880. The reduction in value of q agrees qualitatively with dilute solution measurements. Although at first site the magnitudes of q appear physically unrealistic, it is possible that multiple branches occurred on the highest molecular weight chains leading to a randomly branched structure in which the priority was 7 or more. Read and McLeish[5] have proposed a method for relating the statistical structure derived from the reaction kinetics of metallocene catalysts[9] to an ensemble of pompom modes.

Hence, it is possible that there is an equivalent randomly branched structure in which multiple branches occur on the longest chains. Although the number of branch points per molecule (or 10^4 carbons) associated with a priority of order 10 is considerably higher than the dilute solution measurements suggest, there are assumptions employed in interpreting the dilute solution data concerning the branching density that may not be exactly applicable to these systems.

Ultimately, a wide range of shear and extensional rheological data are required for complete characterization of the model parameters and assessment of the implied molecular structure. Although the fitted model parameters appear to agree with the proposed reaction mechanism for long-chain branching and the dilute solution measurements, they may not be unique. One major consequence of discretizing the relaxation spectrum into a finite set of pompom modes is the loss of uniqueness. Furthermore, the range and quality of rheological data will determine the number and precision of those modes, respectively. In this case, the unusually high number of pompom arms associated with the longest relaxation time could be a result of too few relaxation modes in the range of 10−1000 s. Additional data at longer times or lower frequencies may be required.

Conclusions

The exceptional ability of the multimode differential pompom constitutive model to describe the rheological behavior of various polyethylene structures has been demonstrated. Most notably, the ability to describe the extensional strain-hardening behavior of sparsely branched polyethylenes produced from metallocene catalysts is observed. This represents a unique extension of the pompom constitutive model to sparse, randomly branched materials having an *average* number of branch points per chain less than two. The parameters obtained by fitting of the model to extensional and shear data suggest that multiple branches occur on the longest chains. The rheological contributions to strain hardening from a relatively small fraction of the whole polymer is remarkable.

The model parameters obtained for the sparsely branched polyethylene systems indicate that the separation in the relaxation time scales determines the observed degree of strain hardening. This suggests that the frequency of branch points and not the number of branches, q, at a branch point dominate the extensional rheological response. Not surprisingly, this agrees quite well with the believed mechanism for long-chain branching using constrained-geometry metallocene catalysts. Using the model parameters for the relaxation time scale ratio, the implied degree of long-chain branching for each mPE resin agrees qualitatively with dilute solution measurements. On the other hand, the number of pompom arms associated with the branched pompom modes is unrealistically large. The apparent scaling of q_i with the observed extensional strain-hardening behavior does not agree with the believed long-chain branching mechanism.

Acknowledgment. The authors would like to thank A. Willem deGroot and David Gillespie at the Dow Chemical Co. for providing the LCB and MWD data for all resins presented in this study. The authors would also like to thank T. C. B. McLeish, R. S. Graham, and P. Wapperom for useful discussions regarding the pompom constitutive model.

References and Notes

(1) McLeish, T. C. B.; Larson, R. G. *J. Rheol.* **1998**, *42*, 82−112.
(2) Inkson, N. J.; McLeish, T. C. B.; Harlen, O. G.; Groves, D. J. *J. Rheol.* **1999**, *43*, 873−896.
(3) Blackwell, R. B.; McLeish, T. C. B.; Harlen, O. G. *J. Rheol.* **2000**, *44*, 121−136.
(4) Bick, D. K.; McLeish, T.C. B. *Phys. Rev. Lett.* **1996**, *76*, 2587−2590.
(5) Read, D. J.; McLeish, T.C. B. *Macromolecules* **2001**, *34*, 1928−1945.
(6) Rubenstein, M.; Zurek, S.; McLeish, T. C. B.; Ball, R. C. *J. Phys. (Fr.)* **1990**, *51*, 757−775.
(7) Woo, T. K.; Fan, L.; Ziegler, T. *Organometallics* **1994**, *13*, 2252−2261.
(8) Soares, J. B. P.; Hamielec, A. E. *Macromol. Theory Simul.* **1995**, *4*, 1085−1104.
(9) Soares, J. B. P.; Hamielec, A. E. *Macromol. Theory Simul.* **1997**, *6*, 591−596.

(10) Lai, S. Y.; Wilson, J. R.; Knight, G. W.; Stevens, J. C.; Chum, P. W. S. US Patent No. 5,272,236, 1993.
(11) Schreiber, H. P.; Bagley, E. B. *J. Polym. Sci.* **1962**, *58*, 29−48.
(12) Janzen, J.; Colby, R. J. *J. Mol. Struct.* **1999**, *48*, 569−584.
(13) Wood-Adams, P. M.; Dealy, J. M.; deGroot, A. W.; Redwine, O. D.; *Macromolecules* **2000**, *33*, 7489−7499.
(14) Graessley, W. W.; Raju, V. R. *J. Polym. Sci.: Polym. Symp.* **1984**, *71*, 77−93.
(15) Graessley, W. W.; Masuda, T.; Roovers, J. E. L.; Hadjichristidis, N. *Macromolecules* **1976**, *9*, 127−141.
(16) Raju, V. R.; Rachapuda, H.; Graessley, W. W. *J. Polym. Sci. Phys. Ed.* **1979**, *17*, 1223−1235.
(17) Roovers, J. *Macromolecules* **1984**, *17*, 1196−1200.
(18) Doerpinghaus, P. J. Ph.D. Dissertation, Virginia Tech, Blacksburg, VA, 2002.
(19) Meissner, J. *Pure Appl. Chem.* **1975**, *42*, 553−612.
(20) Bin Wadud, S. E.; Baird, D. G. *J. Rheol.* **2000**, *44*, 1151−1167.
(21) Münstedt, H.; Laun, H. M. *Rheol. Acta* **1979**, *18*, 492−504.
(22) Laun, H. M.; Münstedt, H. *Rheol. Acta* **1978**, *17*, 415−425.
(23) Münstedt, H.; Laun, H. M. *Rheol. Acta* **1981**, *20*, 211−221.
(24) Khan, S. A.; Larson, R. G. *J. Rheol.* **1987**, *31*, 207−234.
(25) Laun, H. M.; Schuch, H. *J. Rheol.* **1989**, *33*, 119−175.
(26) Kasehagen, L. J.; Macosko, C. W. *J. Rheol.* **1998**, *42*, 1303−1327.
(27) Dealy, J. M.; Wissbrun, K. F. *Melt Rheology and Its Role in Plastics Processing: Theory and Applications*; Van Nostrand Reinhold: New York, 1990.
(28) Ye, X.; Sridhar, T. *Macromolecules* **2001**, *34*, 8270−8277.
(29) McLeish, T. C. B.; Allgaier, J.; Bick, D. K.; Bishko, G.; Biswas, P.; Blackwell, R.; Blottiere, B.; Clarke, N.; Gibbs, B.; Groves, D. J.; Hakiki, A.; Heenan, R. K.; Johnson, J. M.; Kant, R.; Read, D. J.; Young, R. N. *Macromolecules* **1999**, *32*, 6734−6758.
(30) Lohse, D. J.; Milner, S. T.; Fetters, L. J.; Xenidou, M.; Hadjichristidis, N.; Mendelson, R. A.; Garcia-Franco, C. A.; Lyon, M. K. *Macromolecules* **2002**, *35*, 3066−3075.
(31) Doi, M.; Edwards, S. F. *The Theory of Polymer Dynamics*; Oxford University Press: Oxford, U.K., 1986.
(32) Axelson, D. E.; Levy, G. C.; Mankelkern, L. *Macromolecules* **1979**, *12*, 41−52.
(33) Kiparissides, C.; Verros, G.; MacGregor, J. F. *Macromol. Chem. Phys.* **1993**, *C33*, 437−527.
(34) Münstedt, H. *J. Rheol.* **1979**, *23*, 421−436.
(35) Bishko, G. B.; Harlen, O. G.; McLeish, T. C. B.; Nicholson, T. M. *J. Non-Newt. Fluid Mech.* **1999**, *82*, 255−273.
(36) Blackwell, R. J.; Harlen, O. G.; McLeish, T. C. B. *Macromolecules* **2001**, *34*, 2579−2596.
(37) McLeish, T. C. B. *Macromolecules* **1988**, *21*, 1062−1087.

MA021332M